Electronic Supplementary Material (ESI) for Physical Chemistry Chemical Physics.

Supplementary Information: A Systematic Study on Immiscible Binary Systems Undergoing Thermal/Photo Reversible Chemical Reactions

Changhao Li, Jianfeng Li,* Hongdong Zhang, and Yuliang Yang†
The State Key Laboratory of Molecular Engineering of Polymers,
Department of Macromolecular Science, Fudan University, Shanghai 200433, China
(Dated: December 5, 2022)

I. EQUILIBRIUM PHASE BEHAVIOR OF AN IMMISCIBLE BINARY SYSTEM UNDERGOING THERMAL REACTIONS

Consider a system consisting of two components A/B interacting with each other at a constant temperature T. The free energy of this system can be written as follow,

$$F = \rho_0 k_\mathrm{B} T \int \mathrm{d}\mathbf{r}[\phi_\mathrm{A} \ln \phi_\mathrm{A} + \phi_\mathrm{B} \ln \phi_\mathrm{B} + \chi \phi_\mathrm{A} \phi_\mathrm{B} \\ + \frac{b}{2}|\nabla \phi_\mathrm{A}|^2 + \phi_\mathrm{A}\epsilon_\mathrm{A} + \phi_\mathrm{B}\epsilon_\mathrm{B}], \tag{S1}$$

where ρ_0 is the total number density of A/B molecules, $\phi_{A/B}$ are the volume fractions of A and B, χ is the dimensionless interaction parameter and b is the gradient energy coefficient. ϵ_A and ϵ_B are the inner energies of A and B in the unit of $k_\mathrm{B}T$, respectively. The chemical potential can be, thus, derived as $\beta\mu_\mathrm{A} = \ln \phi_\mathrm{A} + \chi \phi_\mathrm{B}^2 - b\nabla^2\phi_\mathrm{A} + \epsilon_\mathrm{A}$ and $\beta\mu_\mathrm{B} = \ln \phi_\mathrm{B} + \chi \phi_\mathrm{A}^2 - b\nabla^2\phi_\mathrm{B} + \epsilon_\mathrm{B}$ with $\beta = 1/k_\mathrm{B}T$.

If this binary system is undergoing a thermal reversible reaction $A \rightleftharpoons B$ with the local incompressibility constraint $\phi_\mathrm{A} + \phi_\mathrm{B} = 1$, its dynamical equation is described by Eq. 1 in the main text and its complete form, including noise terms, is given as follow,

$$\frac{\partial \phi_A}{\partial t} = \nabla[D\nabla\frac{\delta F}{\delta \phi_A}] + \alpha(a_B - a_A) + \nabla\cdot\vec{\eta} + \sigma \tag{S2}$$

where $\langle \eta^i(\mathbf{r},t)\eta^j(\mathbf{r}',t')\rangle = 2D\delta^{ij}\delta(\mathbf{r}-\mathbf{r}')\delta(t-t')$, $\langle \sigma(\mathbf{r},t)\sigma(\mathbf{r}',t')\rangle = 2\alpha\delta(\mathbf{r}-\mathbf{r}')\delta(t-t')$, D is the diffusion constant, α is the coefficient for the thermal reaction and $a_{A/B} \equiv \exp(\beta\mu_{A/B})$ are the activities of A and B, respectively, with $\mu_{A/B}$ their chemical potentials and $\beta = 1/k_BT$. These noise terms were mainly introduced by Puri and Oono [1, 2]. σ is the noise term for non-conserved systems (model A), while $\nabla\cdot\vec{\eta}$ is the noise term for conserved systems (model B) [3].

By eq. S2, it is easy to find that the reaction coefficients k_+ and k_- of $A \rightleftharpoons B$ now depend on the local concentrations and can be related to the chemical potentials and α through the following equations,

$$k^+ = \alpha e^{\beta\mu_\mathrm{B} - \ln\phi_\mathrm{B}} \tag{S3}$$

$$k^- = \alpha e^{\beta\mu_\mathrm{A} - \ln\phi_\mathrm{A}} \tag{S4}$$

When there is no chemical reaction ($\alpha = 0$), the equilibrium phase behavior of this system can be obtained by analyzing the free energy density

$$f_\mathrm{sep}(\phi_\mathrm{A}) = k_\mathrm{B}T[\phi_\mathrm{A}\ln\phi_\mathrm{A} + \phi_\mathrm{B}\ln\phi_\mathrm{B} + \chi\phi_\mathrm{A}\phi_\mathrm{B}]. \tag{S5}$$

The binodal line of the binary-blend phase diagram (BBPD) can be obtained by applying the common-tangent construction on $f_\mathrm{sep}(\phi_\mathrm{A})$ while the spinodal line is given by solving $\partial^2 f_\mathrm{sep}(\phi_\mathrm{A})/\partial\phi_\mathrm{A}^2 = 0$.

When there is a thermal reation, the corresponding free energy density is

$$f_\mathrm{therm}(\phi_\mathrm{A}) = k_\mathrm{B}T[\phi_\mathrm{A}\ln\phi_\mathrm{A} + \phi_\mathrm{B}\ln\phi_\mathrm{B} + \chi\phi_\mathrm{A}\phi_\mathrm{B} + \phi_\mathrm{A}\epsilon_\mathrm{A} + \phi_\mathrm{B}\epsilon_\mathrm{B}]. \tag{S6}$$

Simulations have shown that at the late stage of the dynamics, chemical reactions dominate and the final equilibrium state is completely determined by the equation of $a_\mathrm{A} = a_\mathrm{B}$ or $\partial f_\mathrm{therm}(\phi_\mathrm{A})/\partial\phi_\mathrm{A} = 0$. When χ is relatively small

---

* lijf@fudan.edu.cn
† yuliangyang@fudan.edu.cn

and $\epsilon_{\mathrm{A}} \neq \epsilon_{\mathrm{A}}$, there is only one solution to this equation which corresponds to the black solid curve in Fig. 1a in the main text. When χ is relatively big and $\epsilon_{\mathrm{A}} \neq \epsilon_{\mathrm{A}}$, there will be two solutions, one of which corresponds to the metastable state and the black dotted curve in Fig. 1a in the main text. However, if the system is initially near this metastable state, the thermal fluctuation will drive the system to escape from this metastable trap and to evolve to the stable state normally through the nucleation and growth (NG) mechanism followed by spinodal decomposition (SD) mechanism (see Fig. S1-b). Note that, when $\epsilon_{\mathrm{A}} = \epsilon_{\mathrm{B}}$, solutions of this equation will be coincident with the binodal line of BBPD. The dynamical behavior of this case is relatively simple: only phase regions I, II and V in Fig. 1a still exist while others disappear.

II. MORE ON DYNAMICAL PHASE DIAGRAM AND LIGHT SCATTERING OF TPS PATTERNS

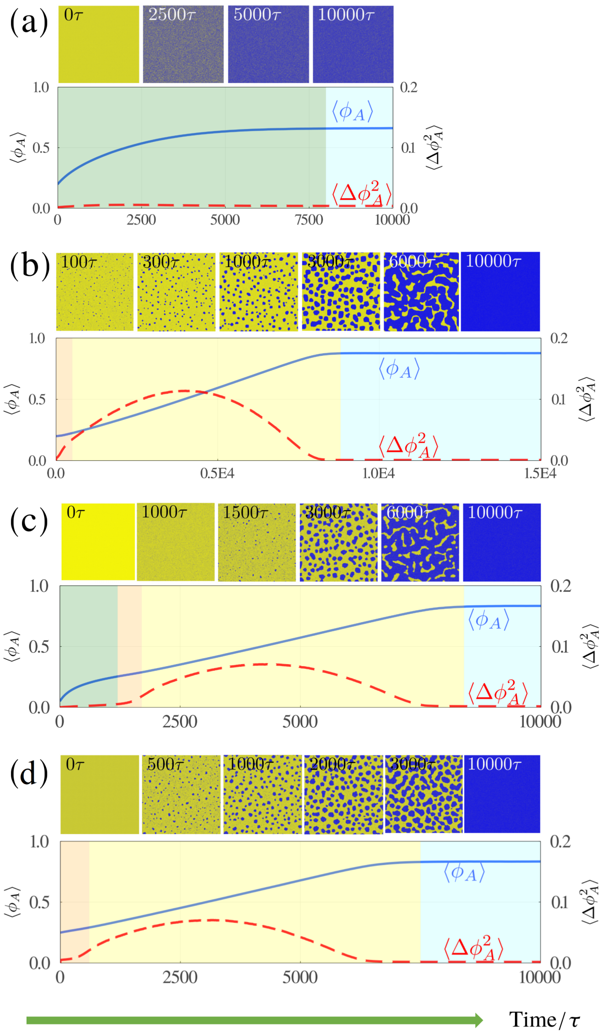

FIG. S1. Snapshots and statistical curves ($\langle\phi_{\mathrm{A}}\rangle \sim t$ and $\langle\Delta\phi_{\mathrm{A}}\rangle \sim t$) of different TPS processes at $\alpha = 0.002$: (a) TPS-V at $\phi_{\mathrm{A,init}} = 0.2$ and $\chi = 1.8$, (b) TPS-III' at $\phi_{\mathrm{A,init}} = 0.2$ and $\chi = 2.5$, (c) TPS-IV at $\phi_{\mathrm{A,init}} = 0.05$ and $\chi = 2.3$ and (d) TPS-IV' at $\phi_{\mathrm{A,init}} = 0.25$ and $\chi = 2.3$.

In Fig. 1 of the main text, typical evolutionary snapshots and statistical curves of TPS-I ($\alpha = 0.002$), II ($\alpha = 0.002$), III ($\alpha = 0.002$) and IV ($\alpha = 0.005$) have been shown. Here, those of TPS-V, III', IV and IV' are shown in Fig. S1 for $\alpha = 0.002$.

As mentioned in the main text, increasing the reaction rate a little bit ($\alpha \sim 0.005$) will render the system difficult to have sufficient time to form nuclei, which will make NG disappear and become UE in some phase regions (II:NG→UE,

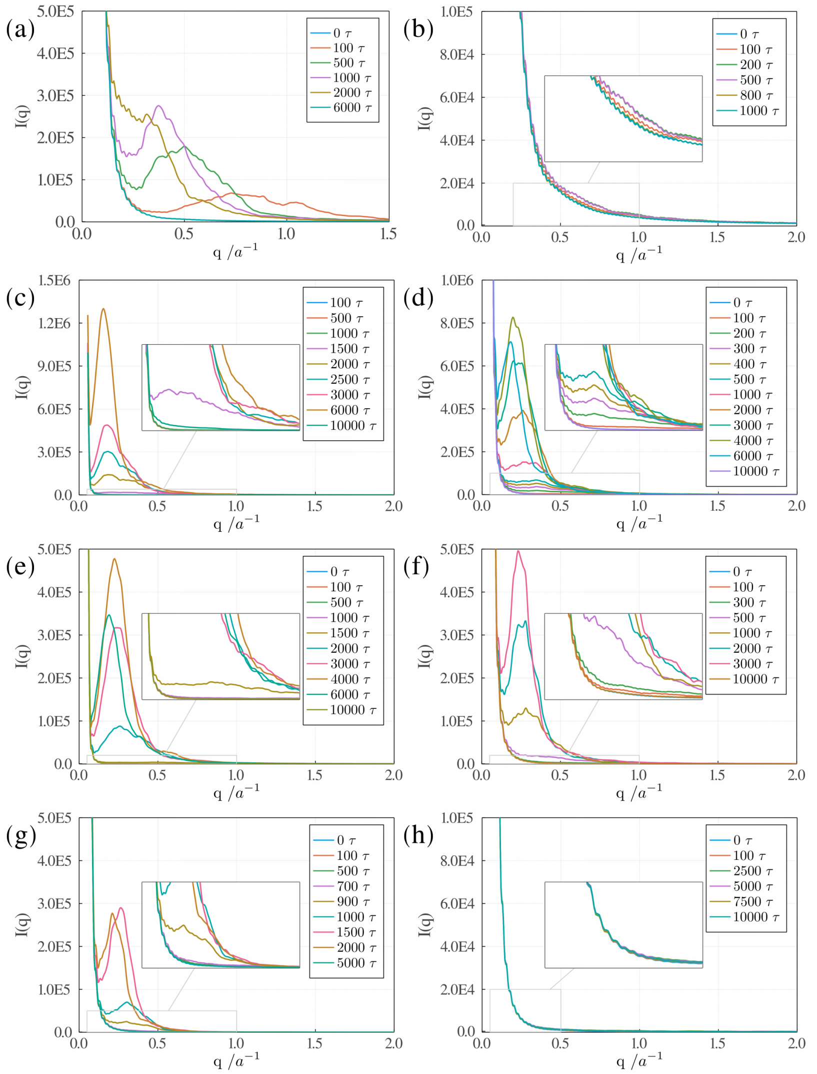

FIG. S2. Light scattering (LS) intensities vs q of patterns at different t. (a) corresponds to Fig. 1b (TPS-I), (b) to Fig. 1c (TPS-II), (c) to Fig. 1d (TPS-III), (d) to Fig. S1-b (TPS-III'), (e) to Fig. S1-c (TPS-IV), (f) to Fig. S1-d (TPS-IV'), (g) to Fig. 1e (TPS-IV at $\alpha = 0.005$) and (h) to Fig. S1-a (TPS-V), respectively. In order to make LS be able to discriminate between uniform evolution (UE), spinodal decomposition (SD), and nucleation and growth (NG), the influence of the mean-concentration has been removed during the calculation of LS. During UE (h), LS curves remain almost the same for different t. During NG (b), LS curves will change with time but remain as a monotonically decreasing function of q. During SD (a), LS curves will have maximums for $q \neq 0$. Note that q is in the unit of $1/a$ with a the lattice size of the simulation.

III': NG-SD→UE-NG-SD, IV:UE-NG-SD→UE-SD and IV':NG-SD→UE-SD). For example, IV:UE-NG-SD→UE-SD means for TPS-IV, UE-NG-SD becomes UE-SD for a bigger α. The transition can be understood as follow. When the reaction rate is extremely small ($\alpha \sim 0.002$), the state started from phase region IV will have sufficient time to form nuclei before its mean concentration crosses the spinodal line and, therefore, TPS under this condition will witness UE, NG and SD successively. On the contrary, when the reaction rate is a little bigger ($\alpha \sim 0.005$), then the system started from phase region IV will not have sufficient time to form nuclei and, therefore, TPS under this condition will only witness UE and SD. However, the phase boundary of this transition is difficult to determine because even for a given α around 0.003, one simulation will probably witness UE-NG-SD while the other might witness UE-SD since the incubation time can be different for two simulations under the same model setting.

Their corresponding light scattering (LS) intensity curves $I(q)$ at different t are shown in Fig. S2. These LS curves are used to further identify, among uniform evolution (UE), spinodal decomposition (SD), and nucleation and growth (NG), which mechanism (process) have been involved for a given temporary phase separation (TPS) process.

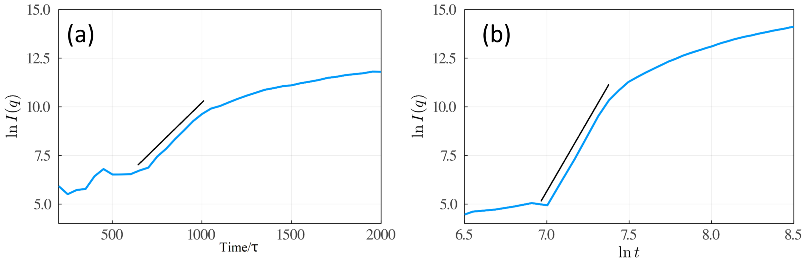

FIG. S3. (a) The $\ln I \sim t$ curve at the fixed q $(= 0.15a^{-1})$ corresponding to Fig. S2-g and Fig. 1e. The black line is a guide to the eyes showing that when spinodal decomposition (SD) is predominant ($t \sim 800$), $I(q)$ does exponentially increase with time [4]. (b) The $\ln I \sim \ln t$ curve at the fixed q $(= 0.15a^{-1})$ corresponding to Fig. S2-c and Fig. 1d. The black line is a guide to the eyes showing that when nucleation and growth is predominant ($\ln t \sim 7.2$), $I(q)$ does increase with time following by a power law [4].

LS functions for UE, SD and NG have the following features [4], respectively. (i) Since $\Delta\phi_{\mathrm{A}}(\mathbf{r}, t) \equiv \phi_{\mathrm{A}}(\mathbf{r}, t) - \langle\phi_{\mathrm{A}}(\mathbf{r}, t)\rangle$ is just the thermal fluctuation of the concentration for a uniform state, LS function of $\Delta\phi_{\mathrm{A}}(\mathbf{r}, t)$ for UE will basically remain the same for different t. (ii) According to Nunes et al.'s work [4], LS curves of NG are monotonically decreasing functions of q and have no maximum for $q \neq 0$. For a given q, I will increase with time following a power law (see Fig. S3-b). (iii) LS curves of SD have maximums for $q \neq 0$ and for a given q, I exponentially increase with time [4] (see Fig. S3-a).

Based on the above three criteria and the LS curves of Fig. S2, we are able to identify what mechanism (process) is predominant at different stages of a given TPS and we present the analysis for the dynamics in the seven phase regions of Fig. 1a, one by one, as follow.

(1) Fig. S2-a and Fig. 1b correspond to TPS-I. Obviously, LS curves of this TPS have maximums at $q > 0$ at the very early stage of the dynamics. Therefore, SD is predominant in TPS-I.

(2) Fig. S2-b and Fig. 1c correspond to TPS-II. LS curves of this TPS have no maximums at $q > 0$ at every stage of the dynamics and for a given q, I does increase with time (see the inset of Fig. S2-b and compare it with that of Fig. S2-h for UE). Therefore, NG is predominant in TPS-II.

(3) Fig. S2-c and Fig. 1d correspond to TPS-III. LS curve at $t = 1000\tau$ (green) is almost overlapped with that at $t = 100\tau$ (cyan), which indicates at the early stage uniform evolution (UE) is predominant. When $1000\tau < t < 2500\tau$, LS curves begin to move 'upwards' but with no maximum for $q \neq 0$ indicating NG is predominant at this stage. When $t > 2500\tau$, LS curves have maximums at $q > 0$ indicating SD is predominant at this stage. Therefore, UE, NG and SD are predominant successively in TPS-III.

(4) Fig. S2-d and Fig. S1-b correspond to TPS-III' at $\alpha = 0.002$. When $t < 200\tau$, LS curves move 'upwards' but with no maximum for $q \neq 0$ indicating NG is predominant at this stage. When $t > 200\tau$, LS curves have maximums at $q > 0$ indicating SD is predominant at this stage. Therefore, NG and SD are predominant successively in TPS-III' at $\alpha = 0.002$.

(5) Fig. S2-e and Fig. S1-c correspond to TPS-IV. LS curves show that UE, NG and SD are predominant successively in TPS-IV at $\alpha = 0.002$.

(6) Fig. S2-f and Fig. S1-d correspond to TPS-IV'. LS curves show that NG and SD are predominant successively in TPS-IV' at $\alpha = 0.002$.

(7) Fig. S2-g and Fig. 1e correspond to TPS-IV at $\alpha = 0.005$. LS curves show that UE and SD are predominant successively in TPS-IV at $\alpha = 0.005$.

(8) Fig. S2-h and Fig. S1-a correspond to TPS-V. LS curves show that UE is predominant in TPS-V for all α.

III. MECHANISM OF MEAN-CONCENTRATION-MOVING TPS

The key to understand the mechanism of MCM-TPS is to show that the phase separation and chemical reactions can be decoupled to some extent at the limit of $\alpha \to 0$ and this can be done in the following linear analysis. Linearizing the dynamical equation (eq. S2) around some given uniform state $\phi_{\mathrm{A}} = \phi_0$ (not necessarily the equilibrium state) or expressing $\phi_{\mathrm{A}}(\mathbf{r})$ as $\delta\phi(\mathbf{r}) + \phi_0$ leads to the following two equations

$$\frac{\partial \delta\phi(\mathbf{k})}{\partial t} = -A\mathbf{k}^4 - B\mathbf{k}^2 - C \qquad \text{(S7)}$$

$$\partial\phi_0/\partial t = \alpha[a_{\mathrm{B}}(\phi_0) - a_{\mathrm{A}}(\phi_0)] \qquad \text{(S8)}$$

where $\delta\phi(\mathbf{k})$ is the Fourier transformation of $\delta\phi(\mathbf{r})$, $A = Db$, $B = D(1/\phi_0(1-\phi_0) - 2\chi) + b\alpha(a_{\mathrm{A}}(\phi_0) + a_{\mathrm{B}}(\phi_0))$ and $C = \alpha(1/\phi_0(1-\phi_0) - 2\chi)(a_{\mathrm{A}}(\phi_0)(1-\phi_0) + a_{\mathrm{B}}(\phi_0)\phi_0)$. Obviously, the first equation describes the initial phase separation dynamics coupled with chemical reaction while the second equation describes the dynamics of the mean concentration ϕ_0 driven by the chemical reaction. At the limit $\alpha \to 0$, it is easy to show that these two equations are approximately independent during a short time period Δt and, thus, the phase separation and chemical reaction can be seen as being decoupled during Δt.

IV. DERIVATION OF EQ. (3) IN THE MAIN TEXT AND EQUIVALENT TEMPERATURE OF LIGHT

The photo reversible reaction $Z \leftrightarrow Z^*$ actually consists of three photo reactions. (I) The molecule in its ground state Z absorbs a photon and transforms into the excited state Z^*: $\nu + Z \to Z^*$; (II) The excited state Z^* spontaneously transforms into the ground state by emitting a photon in a random direction: $Z^* \to Z + \nu$; (III) The excited state absorbs a photon, transits to the ground state and emits two photons in the same direction with the absorbed one: $\nu + Z^* \to Z + 2\nu$ [5]. Obviously, the angular frequency of photons in the above three processes is determined by the energy gap between Z and Z^* as $\omega = \Delta E/\hbar$. For simplicity, we assume that Z and Z^* share the same multiplicity such that the coefficient of absorption, B', and the coefficient of stimulated emission, B, are the same, i.e., $B = B' g_Z/g_{Z^*} = B_0$ with g_Z and g_{Z^*} the mulplicities of Z and Z^*, respectively.

Even though the frequency of photons that can be uniquely determined by ΔE, the sources of these photons can be different carrying different entropies determined by the temperature of the source (see the next section). In this work, we consider two different light sources: one is from a hot blackbody with the temperature T_b and another comes from the background radiant lights of the surrounding environment with the temperature T_s. T_s is also the temperature of the system. For a given point of the system (see Figure S4), it is assumed lights from the blackbody occupies a solid angle of Ω_b while the radiant lights occupies $\Omega_s = 4\pi - \Omega_b$. We introduce solid angles for the following two considerations. First, lights from the external light source usually don't shine on the system in all directions. Second, introdution of the solid angles and the two temperatures (T_b and T_r) is one of possible ways to create two thermal baths corresponding to T_b and T_r which allows the system to stay out-of-equilibrium. In this work, we set $\Omega_b = 0.0046$ and the reason why we choose this parameter such small is that k_r mentioned in the paragraph between eq.(7) and eq.(8) in the main text should not be very large in order to obtain dissipative structures. And the inner energy of transition state M is chosen as $120k_BT_s$ because the common energy of UV light ,say wavelength $\lambda \approx 400$nm, is about $120k_BT$ with T the room temperature $298K$.

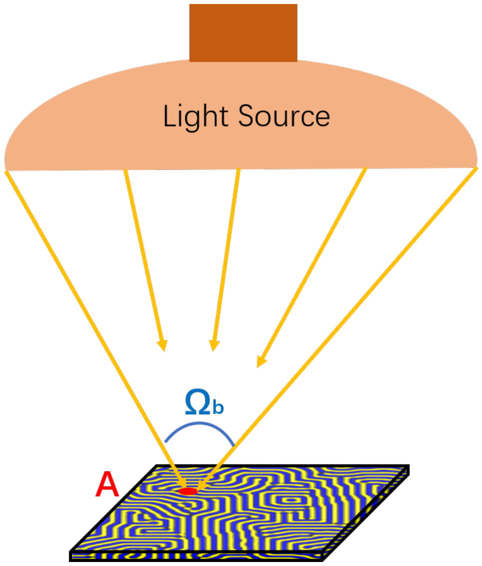

FIG. S4. A demonstration on the introduction of solid angles.

According to the above setting, the transition rates for the above three processes can be written as,

$$\begin{aligned}
r_{\mathrm{I}} &= B_0\phi_Z[I_{T_b,\Omega_b}(\omega)+I_{T_s,\Omega_s}(\omega)] = B_0\phi_Z\frac{\hbar\omega^3}{\pi^2c^3}[\frac{\gamma}{e^{\frac{\hbar\omega}{k_{\mathrm{B}}T_b}}-1}+\frac{1-\gamma}{e^{\frac{\hbar\omega}{k_{\mathrm{B}}T_s}}-1}]\\
r_{\mathrm{II}} &= A\phi_{Z^*} = B_0\phi_{Z^*}\frac{\hbar\omega^3}{\pi^2c^3}[\gamma+(1-\gamma)]\\
r_{\mathrm{III}} &= B_0\phi_{Z^*}\frac{\hbar\omega^3}{\pi^2c^3}[\frac{\gamma}{e^{\frac{\hbar\omega}{k_{\mathrm{B}}T_b}}-1}+\frac{1-\gamma}{e^{\frac{\hbar\omega}{k_{\mathrm{B}}T_s}}-1}]
\end{aligned}$$

where B_0 is the coefficient of stimulated emission, $\gamma=\Omega_b/4\pi$ and $I_{T,\Omega}(\omega)=\frac{\Omega}{4\pi^3c^3}\frac{\hbar\omega^3}{e^{\hbar\omega/k_{\mathrm{B}}/T}-1}$. Note that normally, I_{T_b} will be much bigger than I_{T_s}. These three rates contribute to a change in ϕ_Z as follow,

$$\dot{\phi}_Z = r_{\mathrm{II}}+r_{\mathrm{III}}-r_{\mathrm{I}} = \sum_{x=\{b,s\}} B_0 I_{T_x,\Omega_x}(\omega)(\phi_{Z^*}e^{\frac{\hbar\omega}{k_{\mathrm{B}}T_x}}-\phi_Z) \tag{S9}$$

Therefore, we have derived eq. (3) in the main text and similar results are obtained by Meszéna before [6].

Equivalent temperature of light.–In the above equations, the light source is a blackbody but usually the specific radiation intensity of the light source $I(\omega)$ might not satisfy the distribution $\frac{\hbar\omega^3}{\pi^2c^3[e^{\hbar\omega/k_{\mathrm{B}}/T}-1]}$. However, by solving the equation $I(\omega)=\frac{\hbar\omega^3c^3}{\pi^2[e^{\hbar\omega/k_{\mathrm{B}}/T}-1]}$, one can obtain the equivalent temperature of the light source [7, 8]

$$T(\omega)=\frac{\hbar\omega}{k_B}[\ln(1+\frac{\hbar\omega^3}{\pi^2I(\omega)})]^{-1}. \tag{S10}$$

Thanks to this equivalent temperature, the formulation in the main text is still applicable for all kinds of light sources by simply replacing T_b with $T(\omega)$ in $I_{T_b,\Omega}(\omega)$.

The advantage of using blackbody light source instead of ordinary light source is that the background radiation or heat can be easily considered by another blackbody source but with the system temperature and the solid angle $4\pi-\Omega$ and, in this way, the light source and the background radiation (heat) from the environment can be formulated in the same way.

V. QUANTUM YIELDS OF $A \to B$ AND $B \to A$ REACTIONS

Consider a light source with solid angle Ω_b and the reactions $A \rightleftharpoons A^* \rightleftharpoons B^* \rightleftharpoons B$ with A^* and B^* the excited states of A and B, respectively. If the energy gap and energy barrier between A^* and B^* are both small, then these two excited states can be effectively represented by a single state M and the above reactions can be further simplified to $A \rightleftharpoons M \rightleftharpoons B$. The reaction rate of component A follows,

$$\dot{\phi}_A = r_{\mathrm{II}}^A + r_{\mathrm{III}}^A - r_{\mathrm{I}}^A, \tag{S11}$$

where

$$\begin{aligned}
r_{\mathrm{I}}^A &= B_A\phi_Z[I_{T_b,\Omega_b}(\omega_A)+I_{T_s,\Omega_s}(\omega_A)] = B_A\phi_Z\frac{\hbar\omega_A^3}{\pi^2c^3}[\frac{\gamma}{e^{\frac{\hbar\omega_A}{k_{\mathrm{B}}T_b}}-1}+\frac{1-\gamma}{e^{\frac{\hbar\omega_A}{k_{\mathrm{B}}T_s}}-1}]\\
r_{\mathrm{II}}^A &= A\phi_M = B_A\phi_M\frac{\hbar\omega_A^3}{\pi^2c^3}[\gamma+(1-\gamma)]\\
r_{\mathrm{III}}^A &= B_A\phi_M\frac{\hbar\omega_A^3}{\pi^2c^3}[\frac{\gamma}{e^{\frac{\hbar\omega_A}{k_{\mathrm{B}}T_b}}-1}+\frac{1-\gamma}{e^{\frac{\hbar\omega_A}{k_{\mathrm{B}}T_s}}-1}]
\end{aligned}$$

with $\gamma=\Omega_b/4\pi$ and the reaction rate of B is similar.

Therefore, like the diabatic situation in Penocchio et al.'s work[9], the quantum yield Φ_A of the light reaction $A \to B$ should be as follow,

$$\Phi_A = \frac{r_{\mathrm{II}}^B + r_{\mathrm{III}}^B}{r_{\mathrm{II}}^A + r_{\mathrm{III}}^A + r_{\mathrm{II}}^B + r_{\mathrm{III}}^B} \tag{S12}$$

$$= \frac{B_B\big(\frac{\hbar\omega_B^3}{\pi^2c^3}\big)\big[1+\frac{\gamma}{e^{\frac{\hbar\omega_B}{k_{\mathrm{B}}T_b}}-1}+\frac{1-\gamma}{e^{\frac{\hbar\omega_B}{k_{\mathrm{B}}T_s}}-1}\big]}{B_A\big(\frac{\hbar\omega_A^3}{\pi^2c^3}\big)\big[1+\frac{\gamma}{e^{\frac{\hbar\omega_A}{k_{\mathrm{B}}T_b}}-1}+\frac{1-\gamma}{e^{\frac{\hbar\omega_A}{k_{\mathrm{B}}T_s}}-1}\big]+B_B\big(\frac{\hbar\omega_B^3}{\pi^2c^3}\big)\big[1+\frac{\gamma}{e^{\frac{\hbar\omega_B}{k_{\mathrm{B}}T_b}}-1}+\frac{1-\gamma}{e^{\frac{\hbar\omega_B}{k_{\mathrm{B}}T_s}}-1}\big]}, \tag{S13}$$

and Φ_B for $B \to A$ is similar.

When $B_A = B_B$ and $\omega_A \approx \omega_B$, $\Phi_A \approx \Phi_B \approx \frac{1}{2}$.

VI. ENTROPY PRODUCTION OF THE PHOTO REACTION

Since the total entropy productions of the reactions $A \leftrightarrow M$ and $B \leftrightarrow M$ take the same form, it is sufficient to only consider $A \leftrightarrow M$.

Total entropy production consists of three parts: (i) the entropy production $\dot{S}_I$ due to the light (with $\omega_\mathrm{A} = (E_M - E_\mathrm{A})/\hbar$) absorption and emission; (ii) the entropy production $\dot{S}_{II}$ due to the change of the system's entropy; and (iii) $\dot{S}_{III}$ the entropy production of the environment due to the heat released from the system. Note that in evaluating (iii) the heat due to the photon emission should be excluded.

We divide the concentration change of A into two parts as $\dot{\phi}_A = \dot{\phi}_A^D + \dot{\phi}_A^{\nu,b} + \dot{\phi}_A^{\nu,s}$ where the superscript D denotes the change due to the diffusion of chemicals. $\dot{\phi}_A^{\nu,b} = B_0 I_{T_b,\Omega_b}(\omega_\mathrm{A})[\phi_M e^{\frac{E_M - E_\mathrm{A}}{k_\mathrm{B} T_b}} - \phi_\mathrm{A}]$ and it is similar for for $\dot{\phi}_{A/M}^{\nu,s}$. Then we have

$$\dot{S}_I = \rho_0 \int d\mathbf{r}[\dot{\phi}_A^{\nu,b} \frac{E_M - E_\mathrm{A}}{T_b} + \dot{\phi}_A^{\nu,s} \frac{E_M - E_\mathrm{A}}{T_s} + \dot{\phi}_B^{\nu,b} \frac{E_M - E_\mathrm{B}}{T_b} + \dot{\phi}_B^{\nu,s} \frac{E_M - E_\mathrm{B}}{T_s}]. \tag{S14}$$

$\dot{S}_{II}$ consists of two parts as follow,

$$\begin{aligned} \dot{S}_{II} &= \rho_0 \int d\mathbf{r} \sum_X \frac{\delta S[\phi_{A/B/M}]}{\delta \phi_X} (\dot{\phi}_X^D + \dot{\phi}_X^{\nu,b} + \dot{\phi}_X^{\nu,s}) \\ &= \rho_0 \int d\mathbf{r} \sum_X \frac{\delta S[\phi_{A/B/M}]}{\delta \phi_X} \dot{\phi}_X^D + \rho_0 \int d\mathbf{r} \sum_X \frac{\delta S[\phi_{A/B/M}]}{\delta \phi_X} (\dot{\phi}_X^{\nu,b} + \dot{\phi}_X^{\nu,s}) \\ &= \rho_0 \int d\mathbf{r}[(\ln \phi_M - \ln \phi_\mathrm{A}) \dot{\phi}_A^D + (\ln \phi_M - \ln \phi_\mathrm{B}) \dot{\phi}_B^D] + \rho_0 \int d\mathbf{r} \sum_{X=\{A,B\}} (\ln \phi_M - \ln \phi_X)(\dot{\phi}_X^{\nu,b} + \dot{\phi}_X^{\nu,s}) \end{aligned} \tag{S15}$$

where the free energy of the system $F = H[\phi_{A/B/M}] - T_s S[\phi_{A/B/M}]$.

Similarly,

$$\dot{S}_{III} = -\frac{\rho_0}{T_s} \int d\mathbf{r} \sum_X \frac{\delta H[\phi_{A/B/M}]}{\delta \phi_X} \dot{\phi}_X^D \tag{S16}$$

where the entropy increase of the environment due to the heat released from the system related with photo reaction has been excluded since it has been included in $\dot{S}_I$.

Collecting ν terms in eqs. (S11-S12), we have the total entropy production due to photo reactions as follow,

$$\begin{aligned} \dot{S}_\nu &= \rho_0 k_\mathrm{B} \int d\mathbf{r} \sum_{x=\{b,s\}} \{B_0 I_{T_x}(\omega_\mathrm{A})[\ln \phi_M - \ln \phi_\mathrm{A} \\ &+ \frac{\Delta E_{MA}}{k_\mathrm{B} T_x}](\phi_M e^{\frac{\Delta E_{MA}}{k_\mathrm{B} T_x}} - \phi_\mathrm{A}) + B_0 I_{T_x}(\omega_\mathrm{B})[\ln \phi_M \\ &- \ln \phi_\mathrm{B} + \frac{\Delta E_{MB}}{k_\mathrm{B} T_x}](\phi_M e^{\frac{\Delta E_{MB}}{k_\mathrm{B} T_x}} - \phi_\mathrm{B}).\}. \end{aligned}$$

Therefore, we have derived eq. (10) in the main text.

Collecting D terms in eqs. (S12-S13) leads to eq. (11) in the main text.

[1] Y. Oono and S. Puri, Phys. Rev. A **38**, 434 (1988).

[2] S. Puri and Y. Oono, Phys. Rev. A **38**, 1542 (1988).

[3] A. Onuki, *Phase Transition Dynamics* (Cambridge University Press, 2002).

[4] S. P. Nunes and T. Inoue, J. Membr. Sci. **111**, 93 (1996).

[5] V. B. Berestetskii, E. M. Lifshitz, and L. P. Pitaevskii, *Quantum Electrodynamics: Volume 4* (Butterworth-Heinemann, 1982).

[6] G. Meszéna and H. V. Westerhoff, Journal of Physics A: Mathematical and General **32**, 301 (1999).

[7] H. Ries and A. J. McEvoy, J. Photochem. Photobiol. A: Chem. **59**, 11 (1991).

[8] A. Ore, Phys. Rev. **98**, 887 (1955).

[9] E. Penocchio, R. Rao, and M. Esposito, J. Chem. Phys. **155**, 114101 (2021).